Neurobiology of Disease 130 (2019) 104456

Contents lists available at ScienceDirect

Neurobiology of Disease

journal homepage: www.elsevier.com/locate/ynbdi

Upregulation of tumor necrosis factor-alpha in the anterior cingulate cortex contributes to neuropathic pain and pain-associated aversion

Pei-Wen Yao[a,1], Shao-Kun Wang[a,1], Shao-Xia Chen[a,b], Wen-Jun Xin[a], Xian-Guo Liu[a], Ying Zang[a,*]

[a] Pain Research Center and Department of Physiology, Zhongshan Medical School, Sun Yat-Sen University, 74 Zhongshan Rd. 2, Guangzhou 510080, PR China
[b] Department of Anesthesiology, Sun Yat-Sen University Cancer Center, State Key Laboratory of Oncology in South China, Collaborative Innovation Center for Cancer Medicine, 651 Dongfeng Road East, Guangzhou 510060, PR China

ARTICLE INFO

Keywords:
Tumor necrosis factor-alpha
Neuropathic pain
Pain-associated aversion
Anterior cingulate cortex

ABSTRACT

Injury associated pain involves subjective perception and emotional experience. The anterior cingulate cortex (ACC) is a key area involved in the affective component of pain processing. However, the neuroimmune mechanisms underlying enhanced ACC excitability following peripheral nerve injury are still not fully understood. Our previous work has shown that tumor necrosis factor-alpha (TNF-α) overexpression leads to peripheral afferent hyperexcitability and synaptic transmission potentiation in spinal cord. Here, we aimed to reveal the potential role of ACC TNF-α in ACC hyperexcitability and neuropathic pain. c-Fos, a widely used neuronal activity marker, was induced especially in contralateral ACC early [postoperative (PO) 1 h] and later (PO day 7 and 10) during the development of neuropathic pain. Spared nerve injury (SNI) elevated TNF-α level in contralateral ACC from PO day 5 to 14, delayed relative to decreased ipsilateral paw withdrawal threshold apparent from PO day 1 to 14. Microinjection of anti-TNF-α antibody into the ACC completely eliminated c-Fos overexpression and greatly attenuated pain aversion and mechanical allodynia induced by SNI, suggesting an important role of ACC TNF-α in the pain aversiveness and pain maintenance. Furthermore, modulating ACC pyramidal neurons via a Gi-coupled human M4 muscarinic receptor (hM4Di) or a Gq-coupled human M3 muscarinic receptor (hM3Dq), a type of designer receptors exclusively activated by designer drugs (DREADD), greatly changed the ACC TNF-α level and the mechanical paw withdrawal threshold. The positive interactions between TNF-α and ACC neurons might modulate the cytokine microenvironment thus contribute to the neuropathic pain.

1. Introduction

Pain consists not only of sensory discriminative components relating to location, duration, intensity, and nature of noxious stimuli but also an affective/motivational component associated with unpleasantness or aversion. Anterior cingulate cortex (ACC) neurons receive nociceptive inputs from the thalamus and somatosensory cortices and emotional fear/anxiety signals from the amygdala (Zhuo, 2016). The ACC is the site of integration of sensory inputs and emotional signaling. Evidences increasingly point to a role of ACC in pain processing and pain-related aversion (Chen et al., 2014a; Chen et al., 2018c; Johansen et al., 2001; Koga et al., 2015; Koyama et al., 1998; Tsuda et al., 2017). In the development of neuropathic pain, ACC neuronal hyper-excitability is recognized as an important pathological feature (Blom et al., 2014; Cao et al., 2009; Chen et al., 2018c; Ma et al., 2016; Ning et al., 2013; Zhao et al., 2018). Several lines of evidence suggest that increased excitability in ACC superficial layer (II/III) neurons mainly results from increased excitatory afferent activity following peripheral nerve injury(Li et al., 2010; Ning et al., 2013; Xu et al., 2008). Subsequently, increased ACC excitability may influence the input-output relationship of the inter-cortical network through long-term potentiation (LTP) of synaptic transmission (Chen et al., 2014a; Li et al., 2010). The firing of corticospinal projecting neurons in the ACC deep layers facilitates spinal pain transmission and contributes to the maintenance of behavioral hyperalgesia and allodynia (Chen et al., 2014a; Chen et al., 2018c).

The ACC associated mechanisms underlying behavioral sensitization and pain aversion may be distinct. Drug treatments or genetic manipulations of the ACC that suppress nerve injury-induced behavioral hypersensitivity do not affect pain-related emotional behavior (Gao et al., 2016; Wang et al., 2011; Zhao et al., 2006). It has been

* Corresponding author at: Department of Physiology, Zhongshan Medical School, Sun Yat-Sen University, 74 Zhongshan Rd. 2, Guangzhou 510080, PR China.
E-mail address: zangying@mail.sysu.edu.cn (Y. Zang).
[1] These authors contributed equally to this study.

https://doi.org/10.1016/j.nbd.2019.04.012
Received 14 December 2018; Received in revised form 10 April 2019; Accepted 23 April 2019
Available online 24 April 2019
0969-9961/

suggested that an ACC presynaptic LTP (pre-LTP) requiring increased glutamate release is involved in pain effect while a post-LTP requiring enhanced alpha-amino-3-hydroxy-5-methyl-4-isoxazolepropionic acid (AMPA) receptor activity is involved in behavioral sensitization (Zhuo, 2016). However, the mechanisms underlying enhanced ACC excitability following peripheral nerve injury are still not fully understood.

We previously showed that neuroimmune mechanisms contribute to neuropathic pain associated peripheral nociceptive sensitization (He et al., 2010) and synaptic plasticity in the spinal cord (Liu et al., 2007). Abnormal expression patterns of tumor necrosis factor-alpha (TNF-α), interleukin-1 beta (IL-1β) and interleukin-6 (IL-6) in DRG and spinal cord are responsible for the development of neuropathic pain (Chen et al., 2018a; Chen et al., 2018b; Wei et al., 2013; Wei et al., 2012; Wei et al., 2007; Zang et al., 2015). Increased TNF-α expression leads to peripheral afferent hyperexcitability by triggering over-expression of sodium channels Nav1.3, Nav1.6 and Nav1.8 in dorsal root ganglion (DRG) neurons (He et al., 2010; Zang et al., 2011; Zhang et al., 2018). TNF-α and IL-1β also enhance synaptic transmission by facilitating presynaptic glutamate signaling and postsynaptic NMDA receptor function (Beattie et al., 2002; Viviani et al., 2003). Proinflammatory cytokines may also contribute centrally to neuropathic pain. Increases in TNF-α, IL-1β and IL-6 expression have been described in several supraspinal structures involved in modulating neuropathic pain and these cytokines are implicated in the disease (Al-Amin et al., 2011; del Rey et al., 2011; Detloff et al., 2008; Liu et al., 2017; Ren et al., 2011). However, cytokine expression in pain states has not been extensively investigated in the ACC. In animal models of inflammatory pain, increased ACC TNF-α and IL-1β expression levels were associated with processing in pain-related aversion (Lu et al., 2011), but no prior studies have investigated whether proinflammatory cytokines in the ACC are involved in neuropathic pain processing. In the present study, we observed overexpression of TNF-α in the ACC after peripheral nerve injury and examined the involvement of supraspinal TNF-α in behavioral sensitization and pain affect using a spared nerve injury (SNI) model.

2. Materials and methods

2.1. Animals

Adult male Sprague-Dawley rats (160–220 g) and C57BL/6 mice (20–26 g) were obtained from the Animal Experimental Center, Sun Yat-Sen University, China (License number SCXK (yue) 2008-0002). All procedures were approved by the Animal Care Committee of Sun Yat-Sen University, and were consistent with the National Institutes of Health animal care and ethics guidelines for experimental pain investigations and minimization of animal use and discomfort. Animals were housed in separate cages with controlled humidity, temperature, and 12-h light/dark cycle (06:00–18:00 h). Food and water were available ad libitum.

2.2. Spared nerve injury (SNI)

SNI surgery was performed as previously described (Liu et al., 2007; Wu et al., 2014). Briefly, animals were anesthetized with 0.4% sodium pentobarbital, the skin on the lateral surface of the left thigh was incised and a section was made to expose the sciatic nerve and its three terminal branches: sural, common peroneal and tibial nerves. The common peroneal and tibial nerves were ligated and sectioned (removal of a 2 mm length). The sural nerve was kept intact. The wound was then closed in two layers. In sham-operated rats the nerves were only exposed.

2.3. Mechanical allodynia test

A Dixon up-down method with von Frey hairs was used to measure mechanical allodynia in bilateral rat or mouse hindpaws (Chaplan et al., 1994). Briefly, animals were placed in separate plexiglass chambers positioned on a mesh table and habituated for 15 min prior to testing. Starting with a dose of 2.04 g (rat) or 0.40 g (mouse), von Frey hairs of logarithmically incremental stiffness (rat: 0.41, 0.70, 1.20, 2.04, 3.63, 5.50, 8.51, 15.14 g, or mouse: 0.04, 0.07, 0.16, 0.40, 0.60, 1.0, 1.4, 2.0 g) were applied to the hindpaws. 50% paw withdrawal thresholds were obtained to evaluate response to mechanical stimuli at different postoperative (PO) times.

2.4. Conditioned place aversion (CPA)

CPA experiments were conducted using an automated monitoring system (Jiliang, Shanghai, China). The apparatus consisted of two chambers of the same size ($30 \times 30 \times 53\ cm^3$) separated by a central partition (1 cm thick) with a doorway. One chamber was white with a textured floor while the other was black with a smooth floor. The CPA protocol included pre-conditioning (pre-SNI), conditioning (post-SNI), and testing phases. During preconditioning the animals were habituated to the apparatus for 30 min daily for 3 days (PO-4d to -2d). On PO-1d animals were placed in the white chamber and allowed to move freely in the apparatus for 15 min (3:00–3:15 pm). The percentage of time spent within the black chamber was recorded as the baseline (pre-test). Animals that spent > 80% of the total time in either chamber (approximately 20% of tested animals) were removed from the study. On the next day, the remaining rats received SNI surgery. During the conditioning phase (PO 1d to 10d), mechanical paw withdrawal threshold testing was performed once every two days (9:00–10:00 am) and animals were confined in the black chamber for 30 min. (10:00–10:30 am) each day for 10 days. During the post-SNI testing phase (PO 3, 6, 10d), animals were placed in the white chamber and allowed to move freely in the apparatus for 15 min. (3:00–3:15 pm). Decreased time spent in the black chamber during the testing phase (compared to baseline) indicated avoidance (aversion).

2.5. Immunohistochemistry and immunofluorescence

At designated time points animals were anesthetized and perfused through the ascending aorta with 0.9% saline followed by cold (4 °C) 4% paraformaldehyde in phosphate buffer (PB; 0.1 M sodium phosphate, pH 7.4). Following perfusion brains were removed and postfixed (in the same fixative) for 1 h, then placed in 30% sucrose for 3 days. After dehydration, frozen brain tissue containing ACC (bregma +3.0~ + 1.7 mm) underwent coronal sectioning (25 μm thickness) on a freezing microtome (LEICA CM3050S, Germany).

For immunohistochemistry, sections were first blocked with 3% donkey serum for 1 h at room temperature, then incubated with mouse anti-c-Fos antibody (1:200, Millipore) or rabbit anti-TNF-α antibody (1:200; Bioworld) at 4 °C overnight. After three 10 min PBS washes the sections were incubated with a Cy3-conjugated goat anti-mouse (or anti-rabbit) secondary antibody (1:200; Jackson Immuno Research, USA) for 1 h at room temperature, and then washed in PBS.

For double immunofluorescence staining, the brain sections were incubated with a mixture of anti-TNF-α (1:100; Bioworld) plus either anti-c-Fos (1:100, Millipore), monoclonal neuronal-specific nuclear protein (mouse anti-NeuN; neuronal marker, 1:200; Chemicon, USA), glial fibrillary acidic protein (mouse anti-GFAP, astrocyte marker, 1:200; Chemicon, USA) or mouse anti-Iba1 (microglia marker, 1:200; Millipore) overnight at 4 °C. After three 10 min rinses in PBS, sections were incubated with fluorescein isothiocyanate (FITC)- and Cy3-conjugated secondary antibodies (1:200; Jackson Immuno Research, USA) for 1 h at room temperature, followed by PBS washes.

For imaging, sections were mounted on gelatin-coated slides and air-dried. Images were obtained using a fluorescence microscope attached to a CCD spot camera (LEICA DFC350FX/DMIRB, Germany) and processed with LEICA IM50 software (Germany). To verify specificity of

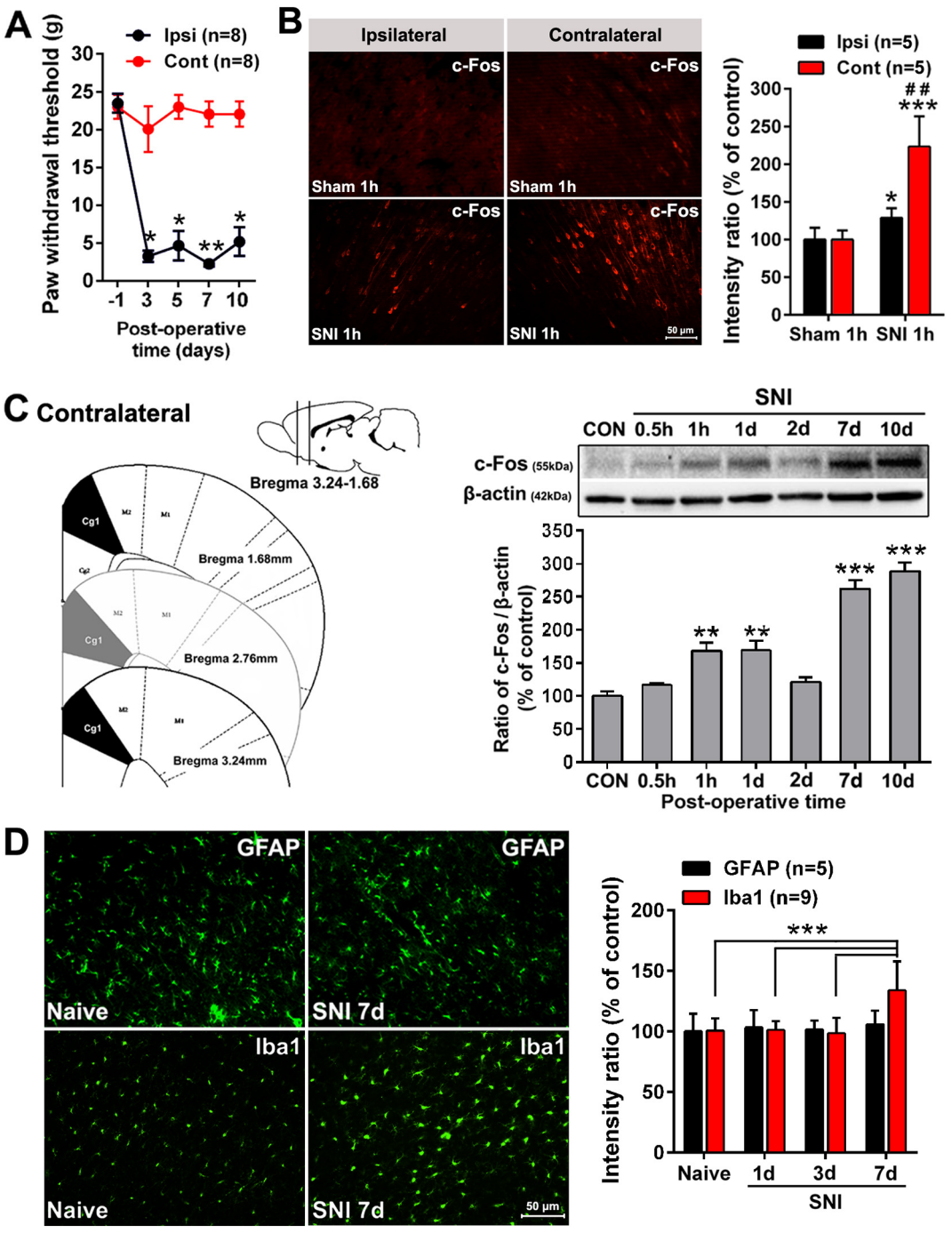

Fig. 1. SNI triggers the activity of ACC neurons. (A) Changes in bilateral mechanical withdrawal thresholds of SNI operated rats. Significant differences were observed in threshold for contralateral paw on day 3, 5, 7 and 10. $n = 8$ rats in each group. Statistical significance was determined by two-way ANOVA. $^{*}p < .05$; $^{**}p < .01$ versus PO -1d. (B)The expression of c-Fos positive ACC neurons after SNI surgery. Representative data obtained from sham and SNI rats was shown. Scale bar = 50 μm. Staining intensity ratio (intensity of ipsilateral or contralateral ACC/intensity of sham operated controls) is shown on the right. $^{*}p < .05$, $^{***}p < .001$ versus sham groups; $^{\#\#}p < .01$ versus ipsilateral side ($n = 5$ rats/group, two-way ANOVA). (C) SNI-induced time course expression for c-Fos protein in contralateral ACC. Left, the tissue of contralateral Cg1 (dark region) was used for western blotting. Sections were in the coronal plane, number in mm anterior to Bregma indicated in this and subsequent figures. Representative western blotting and quantification of c-Fos protein levels in contralateral ACC were shown on the right. Significant differences were observed at earlier (PO 1 h and 1d) and later (PO 7d and 10d) time following SNI. $^{**}p < .01$, $^{***}p < .001$ versus naive control group (n = 5 rats/group, one-way ANOVA).(D) ACC microglia with an activated amoeboid shape was produced 7d after SNI, but no activation of ACC astrocytes was observed on PO 1, 3 and 7d. Left, representative immunofluorescence results of GFAP (astrocyte marker) and Iba1 (microglia marker) in naive controls and SNI rats. Right, quantitation of GFAP (n = 5 rats/group) and Iba1 ($n = 9$ rats/group) immunofluorescence intensity (two-way ANOVA).

the immunostaining and primary antibodies, negative control sections were processed in parallel, but primary antibodies were omitted (data not shown).

2.6. Western blotting

Rats were euthanized at designated time points and tissue samples of ACC were quickly dissected from brain slices (bregma +3.2~ + 1.7 mm) using an anatomical microscope (dark regions in Fig. 1C). Tissue samples were centrifuged at 12,000 rpm for 15 min at 4 °C and proteins were quantified. Proteins were separated by gel electrophoresis (SDS-PAGE) and electro-transferred to a PVDF membrane (Bio-Rad). After blocking with 5% nonfat milk (containing Tris-phosphate buffer, 0.05% T-ween 20) for 1 h at room temperature, the membrane was incubated overnight at 4 °C with mouse anti-c-Fos antibody (1:200; Millipore), polyclonal rabbit TNF-α antibody (1:200; Bioworld), anti-GFAP (1:1000; CST) or anti-Iba1 (1:200; Abcam). Mouse anti-β-actin antibody was used (1:1000, Boster) for gel loading control. The blots were washed three times in TBS-T for 10 min., then incubated with HRP conjugated donkey anti-mouse or anti-rabbit secondary antibodies (1:10000; Abcam). The target protein bands were detected using enhanced chemiluminescence (Bio-Rad) and imaged using a Tanon-5200 Chemiluminescent Imaging System (Tanon Science and Technology). The band intensity of each blot was analyzed by densitometry using an imaging analysis system (KONTRON IBAS 2.0, Germany) and expressed relative to β-actin control.

2.7. Viral injections for the designer receptors exclusively activated by designer drugs (DREADD)

Each animal was deeply anesthetized (1%–2% isoflurane for mouse and 10% chloral hydrate, 0.4 g/kg, i.p. for rat) and then mounted in a stereotaxic frame with nonpuncturing ear bars. pAOV-CaMKIIa-hM4D (Gi)-mCherry-3Flag, pAAV-CaMKIIa-hM3D(Gq)-mCherry or control pAOV-CaMKIIa-mCherry-3Flag and pAAV-CaMKIIa-mCherry (Obio Technology Shanghai Corp., Ltd.; approximate titer 1.0E+12 GC/ml) solution was injected by using a nanoinjector with injection micropipette (Nanoject II Auto-Nanoliter Injector, DRUMMOND, USA) at the following coordinate: anteroposterior (AP) +1.0 mm, mediolateral (ML) 0.2 mm, dorsoventral (DV) -1.2 mm for each mouse; AP +1.5 mm, ML 0.5 mm, DV -2.5 mm for each rat. A total volume of 500 nl for mouse or 2 μl for rat was injected contralaterally at the speed of 23 nl per second. After injection, incisions in the scalp were closed and animals were individually housed for 2 weeks before behavioral tests. Ligand clozapine-N-oxide (CNO) was purchased from Sigma-Aldrich (No.C0832). For experiments in mice, CNO was first dissolved in DMSO and then diluted to a final concentration (5.0 mg/kg) with saline. The final concentration of DMSO was 0.5%. CNO was injected intraperitoneally (i.p.) at a dose of 10 μl/g body weight.

2.8. Intra-ACC drug application

Animals were anesthetized with 10% chloralhydrate (0.4 g/kg, i.p.), and stereotaxic surgery was performed according to the rat brain atlas. A permanent stainless steel guide cannula with a stainless steel stylet plug was inserted into the contralateral ACC of the injured nerve and secured with dental acrylic cement. The stereotaxic coordinate for ACC injection site from bregma was as follows: AP +2.7 mm, ML 0.5 mm, DV-2.5 mm. After surgery, the rats were housed individually and given 1 week to recover from the cannula implantation. Anti-rat TNF-α antibody (AF-510-NA, R&D systems, Inc.) or normal goat IgG control (AB-108-C, R&D systems, Inc.) in two different doses (20 μg/ml or 200 μg/ml, 10 μl, R&D) was injected into the ACC over a 5 min period, 1 day before SNI and once every two days over the course of the following 10 PO days.

2.9. Statistical analysis

For immunohistochemistry, a density threshold above background level was first established to identify positively stained structures. For each animal, ten slices were extracted from a series of consecutive ACC slices (four slice intervals) for statistical analysis. The percentage of positive neurons or immunofluorescence intensity per slice in the same Cg1 region of ACC (300 × 300 pixels) was measured. The intensity ratio relative to the average value of control rats (sham or naive) across the different tissue slices ($n = 10$) from each animal was obtained, and the mean ± SEM across animals ($n = 5$) was determined. All analyses were blinded.

Changes in values over different groups were tested using one-way ANOVA followed by *Dunnett's* multiple comparisons test or using two-way ANOVA followed by *Sidak's* multiple comparisons test. For behavioral testing data, nonparametric two-way ANOVA followed by *Friedman* test was employed. In all cases, $p < .05$ was considered statistically significant. The n number indicates number of animals.

3. Results

3.1. ACC hyperexcitation was responsible for mechanical allodynia

Consistent with earlier findings (Tan et al., 2015), we confirmed that unilateral SNI induced a long-lasting decrease in ipsilateral paw withdrawal thresholds ($p < .05$) from PO day 3 to day 10 (Fig. 1A). To confirm changes in neuronal excitability in the ACC after SNI surgery, we first examined the immunoreactivity (IR) of c-Fos, a widely used activity marker (Wei et al., 2002). No c-Fos-IR positive neurons were observed at PO 1 h in sham operated control rats. SNI induced increases of c-Fos-IR in ACC to greater and lesser extents (compared to sham operated controls) in contralateral ($p < .001$) and ipsilateral ($p < .05$) sides, respectively (Fig. 1B). Further analysis by western blotting focused on the contralateral ACC and showed that c-Fos level was significantly increased at PO 1 h, representing an immediate response to SNI surgery because c-Fos expression usually peaks 60–90 min after stimulation ($p < .001$) and 1d ($p < .001$), returned to naive control levels at PO 2d, then dramatically increased at PO 7d and 10d ($p < .001$, Fig. 1C). Furthermore, to eliminate potential impact of prelimbic cortex, we performed another experiment by using bregma 1.2–0 mm (where Cg1/Cg2 is present) as a test site. The data showed that the expression pattern of ACC c-Fos (Supplementary Fig. 1) in this area was similar to that shown in Fig. 1C. Sham operation had no significant effects on c-Fos expression. Above results suggested that c-Fos expression was induced early by nerve injury and also later during the development of neuropathic pain (Tan et al., 2015).

Here, we also tested the potential roles of ACC glial cells in neuropathic pain. Immunofluorescence analysis of GFAP (astrocyte marker) and Iba1 (microglia marker) in naive control rats and SNI-operated rats showed activation of microglia with amoeboid shape in contralateral ACC 7d after SNI but no activation of astrocytes 1, 3 and 7d after SNI (Fig. 1D).

Our above results suggest that pain-related ACC activity may be mediated mainly by neurons following SNI surgery. To confirm this hypothesis, we tested whether the activity of ACC excitatory pyramidal neurons plays a causative role in mechanical allodynia observed in SNI model. To modulate the activity of ACC neurons, we used DREADD-hM4Di or hM3Dq (hM4Di, Gi-coupled human M4 muscarinic receptor; hM3Dq, Gq-coupled human M3 muscarinic receptor), which couples through a Gi or Gq pathway to hyperpolarize or depolarize neuronal membrane potential upon the application of synthetic ligand CNO. To selectively express hM4Di or hM3Dq in ACC excitatory pyramidal neurons, the pAOV-CaMKIIa-hM4D(Gi)-mCherry-3Flag (hM4Di-mCherry) or pAAV-CaMKIIa-hM3D(Gq)-mCherry (hM3Dq-mCherry) was injected into the contralateral (right) ACC of mice with or without SNI surgery, respectively. As shown in Fig. 2A, mCherry was

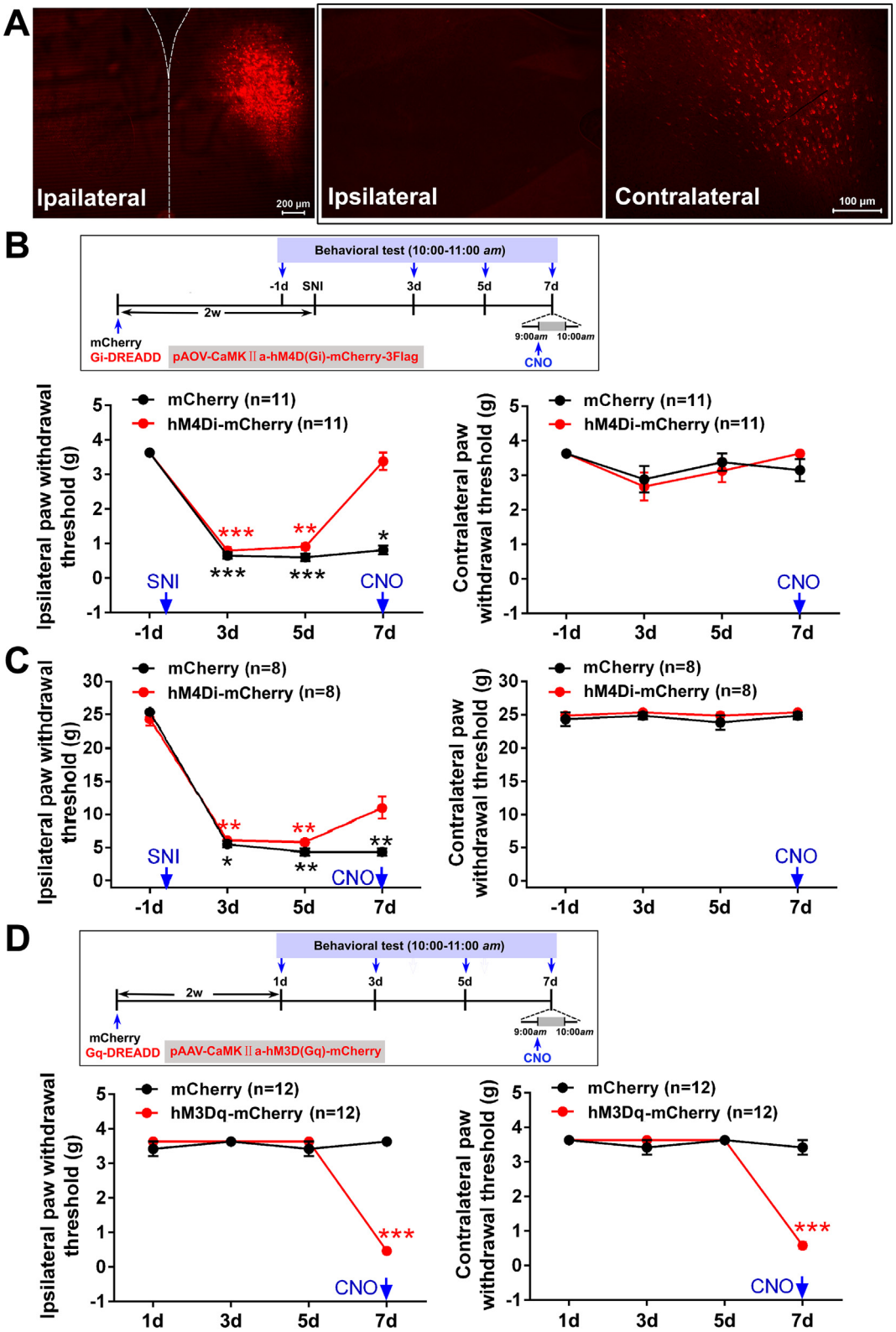

Fig. 2. Modulating activities of ACC pyramidal neurons using DREADD- hM4Di or hM3Dq affect the mechanical paw withdrawal thresholds. (A) The injecting site of virus carrying hM4Di-, hM3Dq-mCherry or mCherry in contralateral ACC (left). Enlarged images from bilateral ACC were shown on the right. (B) Behavioral test paradigm and the effect of DREADD-hM4Di on mechanical paw withdrawal thresholds inmice/rats with SNI surgery. Compared to the mCherry control mice, DREADD-hM4Di reversed the SNI-induced decrease of ipsilateral threshold but did not affect the base line in contralateral side. $^{*}p < .05$, $^{**}p < .01$, $^{***}p < .001$ versus PO -1d ($n = 11$ mice/group, two-way ANOVA). (C) Compared to the mCherry control rats, DREADD-hM4Di relieved the decrease level of ipsilateral threshold induced by SNI. $^{*}p < .05$, $^{**}p < .01$, $^{***}p < .001$ versus PO -1d ($n = 8$ rats/group, two-way ANOVA). (D) Behavioral test paradigm and the effect of DREADD-hM3Dq on paw withdrawal thresholds in mice without any nerve injury. DREADD-hM3Dq induced significant decrease of threshold in bilateral hind paws. $^{***}p < .001$ versus 1d ($n = 12$ mice/group, two-way ANOVA).

specifically detected in the Cg1 region of contralateral ACC but no expression in other brain regions. In parallel, all control mice received contralateral injections of pAOV-CaMKIIa-mCherry-3Flag or pAAV-CaMKIIa-mCherry (Fig. 2B, C).

To examine the effect of inhibiting the activity of ACC pyramidal neurons on mechanical allodynia, SNI surgery was performed on mice 2 weeks after hM4Di-mCherry virus injection and CNO (5.0 mg/kg) was administrated i.p. at PO 7d (Fig. 2B). The ipsilateral decreased paw withdrawal threshold was reversed 1 h after injection of CNO ($p > .05$, compared with that tested at PO -1d). Conversely, in control mice injected with mCherry virus, same dose treatment of CNO did not affect the SNI-induced allodynia, the paw withdrawal threshold was still at a lower level compared with the base line (PO -1d, $p < .05$). On the contralateral side, no mechanical allodynia was produced and no changes were found in both mCherry control group and hM4Di-mCherry group after CNO injection. Using the same method on rats, we obtained similar results although the decreased paw withdrawal threshold by SNI was not completely reversed to the base line following administration of CNO (Fig. 2C).

To further test the role of ACC in pain behavior, we used DREADD-Gq to enhance the excitability of ACC. As shown in Fig. 2D, behavioral test was performed once every 2 days from 2 weeks after hM3Dq-mCherry injection and CNO (5.0 mg/kg) was injected into the normal mice 1 h before the 4th behavioral test (7d). The data indicated that administration of CNO dramatically decreased the paw withdrawal thresholds on both sides ($p < .001$), and the decreased amplitudes were similar to those observed in SNI mice. The induction of ACC hyperexcitation contributed to the mechanical allodynia.

3.2. TNF-α triggered ACC hyperexcitation thus contributed to the SNI-induced pain aversion and behavioral hypersensitivity

We analyzed bilateral TNF-α-IR and found that it was increased significantly in contralateral but not ipsilateral ACC at PO 10d (Fig. 3A). IR quantitative analysis revealed a striking increase in TNF-α-IR in contralateral ACC of SNI treated rats ($p < .001$, Fig. 3B). Western blot analysis of contralateral ACC showed elevated TNF-α levels at PO 5d ($p < .01$), 7d ($p < .001$) and 14d ($p < .05$, Fig. 3C), delayed relative to decreased ipsilateral paw withdrawal threshold apparent from PO 1d to 14d (Fig. 3D), suggesting a potential maintenance but not inductive role of TNF-α in neuropathic pain.

Dual immunolabeling studies were performed to identify the cells responsible for TNF-α upregulation in ACC. TNF-α colocalized with NeuN (neuronal marker), but not GFAP or Iba1 7d after SNI (Fig. 4A). Furthermore, about 33% of TNF-α positive neurons were strikingly colocalized with c-Fos positive neurons at PO 10d but not PO 5d (Fig. 4B). After nerve injury, the contralateral c-Fos was first increased at PO 1 h and 1d, then re-upregulated at PO 7d and PO 10d (Fig. 1D). No significant change of c-Fos protein level was observed at either PO 3d or PO 5d (Fig. 4C). However, the contralateral increase of TNF-α was able to be detected 5d after SNI (Fig. 3C and Fig. 4C). These results raise the possibility that TNF-α overexpression may be involved in the c-Fos

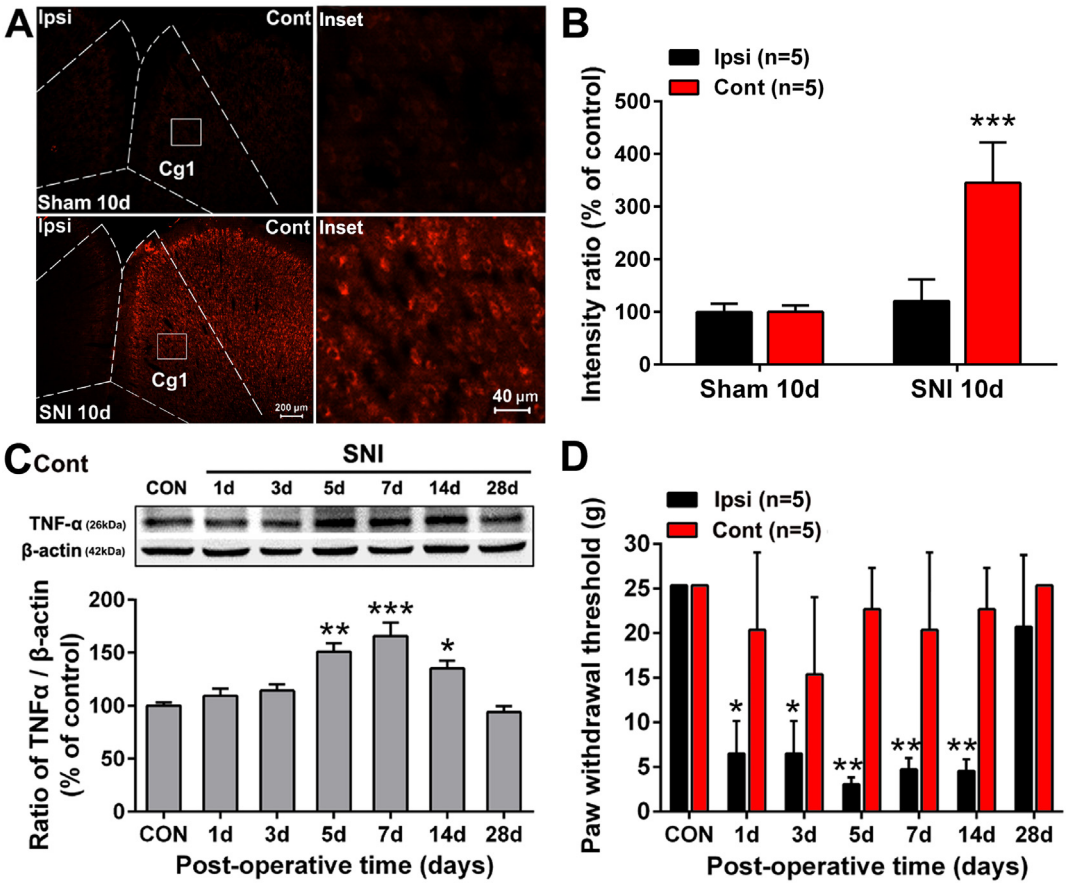

Fig. 3. SNI induces TNF-α upregulation in contralateral ACC. (A) Distribution of TNF-α-IR staining neurons in both sides of ACC comparing to sham (top) and SNI (below) operated rats. Dashed lines indicate the region of Cg1. Higher magnification micrographs from boxed areas were shown on the right. (B) Quantification of immunofluorescence intensity in bilateral ACC indicated striking increase of TNF-α-IR on the contralateral side 10d after SNI surgery. ***$p < .001$ versus sham group (n = 5 rats/group, two-way ANOVA). (C) Western blotting and quantification showed that TNF-α protein levels increased at5d, 7d and 14d after SNI. *$p < .05$, **$p < .01$, ***$p < .001$ versus naive control rats (n = 5 rats/group, one-way ANOVA). (D) Quantification of mechanical paw withdrawal thresholds in each group of animals. The contralateral thresholds were decreased significantly on days 1, 3, 5, 7, and 14, preceded by the change of ACC TNF-α. *$p < .05$, **$p < .01$ versus naive control group (n = 5 rats/group, two-way ANOVA).

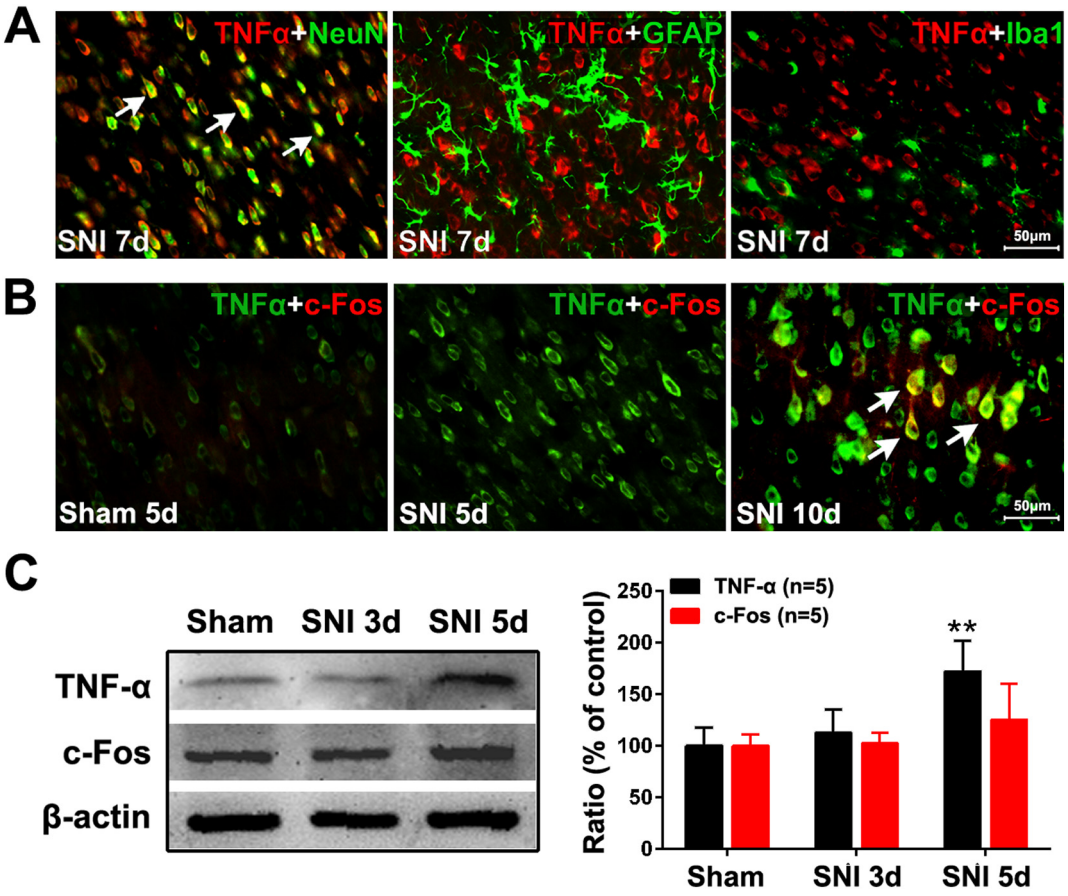

Fig. 4. SNI-induced TNF-α is expressed in ACC neurons and c-Fos positive cells. (A) Double immunofluorescence staining showed that TNF-α-IR (red) was co-localized with NeuN (neuronal marker, green), but not GFAP (astrocyte marker, green) and Iba1 (microglia marker, green) 7d after SNI. (B) Upregulated TNF-α-IR (green) after SNI co-localizes with c-Fos-IR (red) on PO 10d. No significant signals of TNF-α and c-Fos were observed in sham rats and no positive c-Fos-IR on PO 5d following SNI. (C) Western blotting and quantification showing increase of TNF-α protein level on day 5, but not c-Fos either day 3 or 5 after SNI. $^{**}p < .01$ versus sham group (n = 5 rats/group, two-way ANOVA). (For interpretation of the references to colour in this figure legend, the reader is referred to the web version of this article.)

re-upregulation, contributing to the maintenance of ACC hyperexcitability during the development of neuropathic pain.

To test the role of ACC TNF-α on SNI-associated pain behaviours including pain-related aversion and behavioral hypersensitivity, we first used CPA to induce pain aversion in SNI treated rats (Fig. 5A, B). We then measured the effects of neutralization of endogenous ACC TNF-α by antibody administration on c-Fos expression as well as SNI-associated pain behaviours. As shown in Fig. 5B, CPA decreased the percent of time spent in the black chamber (compared to pre-operation baseline), indicating aversion, at PO 10d ($p < .01$) but not at 3d and 6d. Micro-injection of anti-TNF-α antibody (200 μg/ml, 10 μl) but not the same dose of IgG (data not shown) into the ACC 1 day before SNI and once every two days until PO 9d (Fig. 5C) completely eliminated upregulation of c-Fos protein 10d after SNI (Fig. 5D). In behavioral tests, low dose anti-TNF-α (20 μg/ml, 10 μl) micro-injection into ACC greatly attenuated pain aversion induced by SNI surgery (Fig. 5E), but only mildly increased mechanical paw withdrawal threshold (Fig. 5F). Increasing anti-TNF-α antibody dose to 200 μg/ml (10 μl) highly attenuated both pain aversion and mechanical allodynia induced by SNI (Fig. 5G, H).

Furthermore, as shown in Fig. 3, TNF-α was upregulated 10d after SNI in other cortical areas including M1and M2. To exclude the effect of TNF-α in these motor cortices, TNF-α antibody (200 μg/ml, 10 μl) was administered into M2/M1 areas by using the same injection method. We found that TNF-α inhibition in M2/M1 also blocked the induction of mechanical allodynia and pain aversion by SNI.

3.3. Effects of modulation of ACC neuronal activities on TNF-α expression

The above results indicated that SNI surgery induced ACC TNF-α overexpression, which contributed to the development of neuropathic pain through triggering ACC hyperexcitation. In this process, whether activated ACC neurons, in turn, increase TNF-α expression thus contribute to the cytokines microenvironmental disorders remains to be elucidated.

We used DREADD-Gq or DREADD-Gi to promote or inhibit the activities of ACC pyramidal neurons respectively, and then examined the effects of modulating ACC activities on TNF-α expression. As shown in Fig. 6A, SNI surgery (SNI+) was performed 2 weeks after the injection of virus carrying hM4Di-mCherry while no any nerve injury (SNI-) was given to those mice injected with hM3Dq-mCherry. The control mice received the virus carrying mCherry only. On the 7th day following SNI +/−, behavioral tests were performed 0.5 h before and after CNO (5.0 mg/kg) treatment. After behavioral tests, bilateral ACC were immediately dissected from brain and used to test c-Fos and TNF-α expression levels by western blotting. Similar to the results shown in Fig. 2, administration of CNO decreased bilateral paw withdrawal thresholds in the normal mice receiving hM3Dq virus ($p < .01$) but reversed the SNI-induced allodynia in mice injected with hM4Di (Fig. 6B). Western blotting for c-Fos confirmed the changes in ACC activities following application of DREADD-Gq or Gi (Fig. 6C). Similar to c-Fos expression pattern, TNF-α in ACC was increased bilaterally in mice with DREADD-Gq ($p < .001$) and decreased contralaterally in SNI

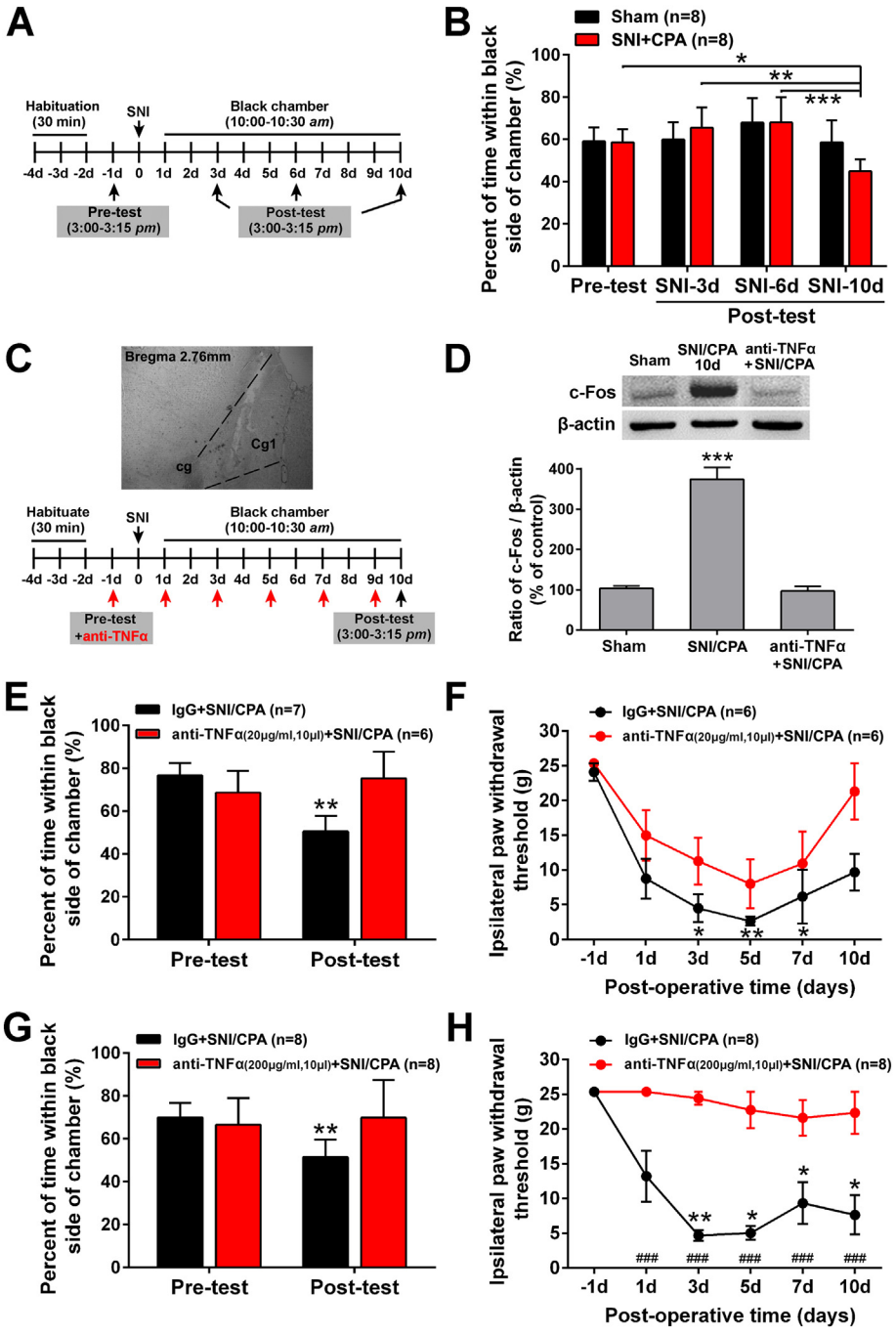

Fig. 5. Microinjection of TNF-α antibody into ACC blocks the induction of pain aversion by CPA following SNI and attenuates the behavioral hypersensitivity. (A) The schema for CPA method used to induce pain-related aversion in SNI-operated rats. (B) The time spent in the black chamber was reduced after CPA training on PO 10d following SNI, indicating a successful induction of pain aversion. $^{*}p < .05$, $^{**}p < .01$, $^{***}p < .001$ (n = 8 rats/group, two-way ANOVA). (C) The mark left by the cannula implantation showing the drug injecting site in Cg1 region. Behavioral test and drug (anti-TNF-α antibody) administration schema is shown in a lower panel. (D) Western blotting showing the inhibitory effect of anti-TNF-α antibody (200 μg/ml, 10 μl) on the increased c-Fos protein level induced by CPA following SNI surgery at day 10. $^{***}p < .001$ versus sham group (n = 5 rats/group, one-way ANOVA). (*E*-F) Percentage of time spent in the black chamber and changes in mechanical paw withdrawal threshold with low dose TNF-α antibody (20 μg/ml, 10 μl). $^{*}p < .05$, $^{**}p < .01$ versus pre-test or -1d ($n = 6$ rats/group, two-way ANOVA). (G-H) Percentage of time spent in the black chamber and changes in mechanical withdrawal threshold with high dose TNF-α antibody (200 μg/ml, 10 μl). $^{*}p < .05$, $^{**}p < .01$ versus pre-test or -1d; $^{\#\#\#}p < .001$ versus IgG control group (n = 8 rats/group, two-way ANOVA).

mice with DREADD-Gi ($p < .01$, Fig. 6D), confirming that the activities of ACC pyramidal neurons were able to modulate the expression of TNF-α.

Furthermore, it has been reported that the induction of pain-related aversion triggers the ACC TNF-α overexpression in an inflammatory pain model (Lu et al., 2011). Here, we also tested the effects of pain aversion on ACC c-Fos, TNF-α and SNI-induced allodynia. Compared to the sham operated control groups, at PO 10d SNI increased contralateral c-Fos-IR and TNF-α-IR, the former mainly localized in the deep ACC layers V and the latter widely distributed in layers II to VI (Fig. 7A-D). The induction of pain aversion by CPA following SNI (Fig. 7F) enhanced the IR of c-Fos but not TNF-α in layers V in as compared to SNI treatment only ($p < .001$, Fig. 7C, D). Western blotting further confirmed that the induction of pain aversion after SNI increased contralateral c-Fos level in ACC ($p < .05$ versus SNI treatment group, Fig. 7E). However, CPA did not significantly enlarged the amplitude of the decreased paw withdrawal threshold induced by SNI (Fig. 7G), suggesting that increase of c-Fos but no TNF-α is insufficient to affect the behavioral hypersensitivity.

4. Discussion

In this work, we showed that SNI surgery induced TNF-α upregulation in contralateral ACC which was delayed relative to the pain induction. Microinjection of TNF-α antibody into the ACC completely eliminated c-Fos upregulation, and greatly attenuated pain aversion as well as mechanical allodynia, suggesting that ACC TNF-α is important in the pain aversiveness and pain maintenance. Moreover, ACC modulation by DREADD-Gq or Gi also affected ACC TNF-α level and pain threshold of the paw to the mechanical stimuli. The interaction between

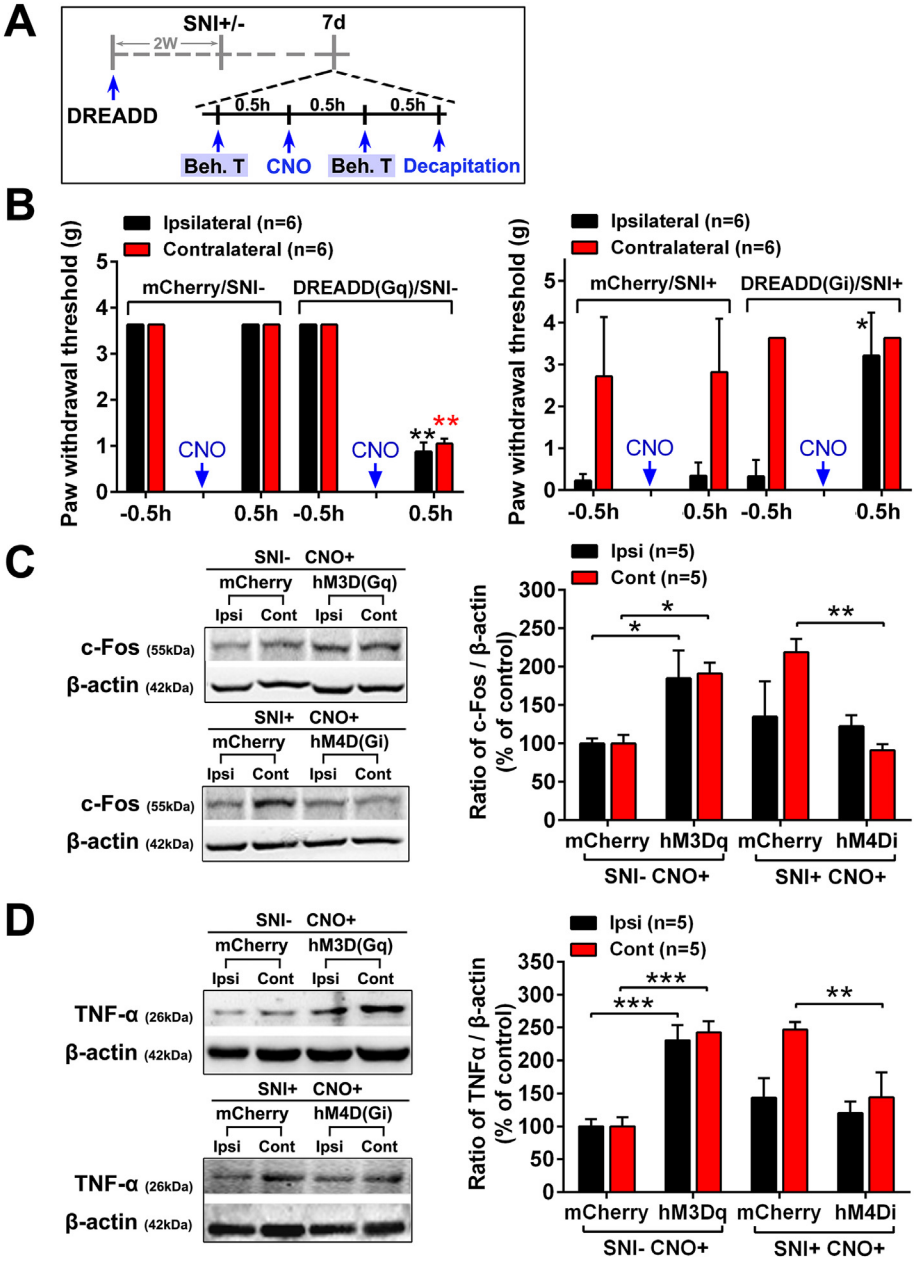

Fig. 6. Effects of DREADD-hM3Dq and hM4Di on ACC c-Fos and TNF-α protein levels. (A) The schema for behavioral test (B) The effects of DREADD-hM3Dq (Gq) or hM4Di (Gi) on mechanical paw withdrawal thresholds in mice without SNI or with SNI surgery, respectively. $^{*}p < .05$, $^{**}p < .01$ versus −0.5 h (n = 6 rats/group, two-way ANOVA). (C) Western blotting and quantification for bilateral and contralateral c-Fos in the mice injected with DREADD-Gq and DREADD-Gi, respectively. $^{*}p < .05$, $^{**}p < .01$ versus mCherry control groups (n = 5 rats/group, two-way ANOVA). (D) Western blotting and quantification for bilateral TNF-α in the mice injected with DREADD-Gq and DREADD-Gi, respectively. $^{*}p < .05$, $^{**}p < .01$, $^{***}p < .001$ versus mCherry control groups (n = 5 rats/group, two-way ANOVA).

TNF-α and ACC neurons might change the cytokine microenvironment thus contributes to the neuropathic pain.

4.1. SNI triggers pyramidal neuron activity in ACC deep layers

Spinal nociceptive transmission is under biphasic modulation from supraspinal structures (Heinricher et al., 2009), especially brainstem-spinal descending facilitatory modulation (Urban and Gebhart, 1999; Urban et al., 1999). The ACC can affect spinal nociceptive transmission directly through the top-down ACC-SDH facilitatory systems (Chen et al., 2014a; Chen et al., 2018c). Pyramidal neurons in the ACC deep layers (V yr) send direct descending projecting terminals to the ACC-spinal dorsal horn (SDH) (lamina I-III) with a contralateral preference, and these descending projection cells can be activated by peripheral nerve injury (Chen et al., 2014a). Meanwhile, direct ACC electrical stimulation also facilitates the synaptic transmission of spinal cord by exciting the projecting neurons and excitatory interneurons in SDH (Chen et al., 2018c). In this work, we observed that unilateral SNI induced bilateral increases of c-Fos-IR in rat ACC, especially on contralateral side, at PO 1 h (Fig. 1B). The increased c-Fos-IR was localized mainly in the deep layer V/VI (Fig. 7A and C). Further analysis of contralateral ACC showed that c-Fos was significantly increased at PO 1 h and 1d, returned to control levels at PO 2d, and then showed a robust increase at PO 7d and 10d (Fig. 1C). Individual ACC neuron can respond to acute noxious stimuli by increasing firing rate (Kuo and Yen, 2005; Zhang et al., 2017), and the frequency of spontaneous membrane-potential oscillations of ACC neurons is enhanced significantly within 7 to 14 days after nerve injury (Ning et al., 2013). Therefore, early ACC neuron excitability up to PO 1d after nerve injury might be due to the excitatory afferent activity from the peripheral nociceptive system, while the synaptic plasticity in ACC triggered by persistent nociceptive inputs could account for the later increase of c-Fos started at PO 7d.

Interactions between neurons and glial cells are reportedly important in neuropathic pain (Tsuda et al., 2017). ACC neuronal hyperexcitability plays a pivotal role in pain processing, but the roles of ACC astrocytes and microglia in neuropathic pain remain unclear. It has been suggested that activation of ACC glial cells is time-dependent and/

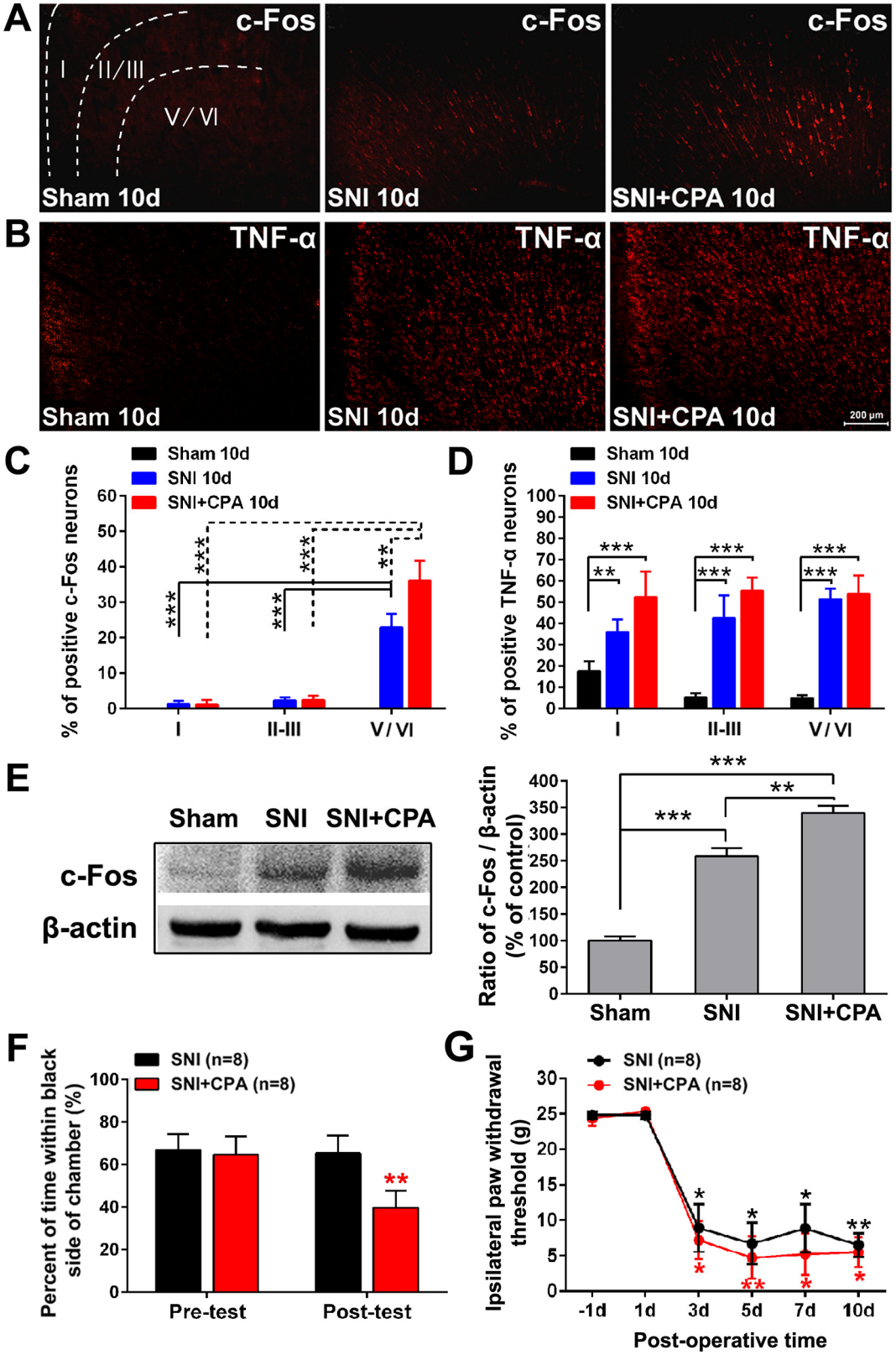

Fig. 7. SNI plus CPA increases excitability of ACC neurons without significant effects on ACC TNF-α expression and mechanical paw withdrawal threshold. Coronal slices showed the immunofluorescence labeling of c-Fos (A) and TNF-α (B) in sham operated controls, SNI rats and CPA induced SNI rats. Dotted lines indicate the bottom of different layers of the ACC cortex. The percentage of positive neurons for c-Fos (C) and TNF-α (D) in contralateral ACC showed that the signal of neuronal activity marker localizes to the deep layer V/VI and TNF-α is widely distributed in every layers. The c-Fos-IR but not TNF-α in layers Vin is increased by CPA, as compared to the SNI rats. $^{**}p < .01$, $^{***}p < .001$ (n = 5 rats/group, two-way ANOVA). (E) Western blotting and quantification showed a more striking increase of c-Fos protein level in CPA induced SNI rats. $^{**}p < .01$, $^{***}p < .001$ (n = 5 rats/group, one-way ANOVA). (F) Percentage of time spent in the black chamber after CPA induction was significantly different from SNI rats at PO 10d. $^{**}p < .01$ versus pre-test (n = 8 rats/group, two-way ANOVA). (G) No significant difference was observed in the mechanical paw withdrawal threshold between SNI group and CPA induced SNI group. $^{*}p < .05$, $^{**}p < .01$ versus -1d (n = 8 rats/group, two-way ANOVA).

or may differ among chronic pain experimental models (Tsuda et al., 2017). GFAP-IR and Iba1-IR are upregulated in the ACC in sciatic nerve ligation experiments (Kuzumaki et al., 2007; Miyamoto et al., 2017; Narita et al., 2006). However, neither GFAP-IR nor Iba1-IR was increased in ACC of SNI or common peroneal nerve ligation mouse models (Ikeda et al., 2013; Zhang et al., 2008). Microglia are not activated by neuronal activity and LTP in brain slices (Wu and Zhuo, 2008) and both post-LTP and pre-LTP are insensitive to minocycline that inhibits microglial activation in the ACC (Song et al., 2015). Furthermore, our current study in rats showed that activation of microglial cells in ACC only occurred at 7d and no any changes in astrocyte 1, 3 and 7d after SNI (Fig. 1D). SNI-induced TNF-α was mainly co-localized with NeuN positive neurons (Fig. 4A). Thus, it is very likely that pain-related ACC activity was mainly mediated by neurons in our SNI model.

Recent optogenetics studies involving modulation of ACC neuronal activity revealed pivotal roles of ACC excitatory pyramidal neurons in nociception and pain affect in chronic inflammatory pain models (Kang et al., 2017; Zhang et al., 2017) and SNI neuropathic pain model (Chen et al., 2018c). In this work, modulation of ACC neuronal activity by DREADD-Gq or Gi directly decreased bilateral paw withdrawal threshold to mechanical stimuli in normal mice or reversed ipsilateral mechanical allodynia in SNI mice/rats (Fig. 2), further confirming that ACC may affect spinal nociceptive transmission.

4.2. SNI-induced TNF-α overexpression promoted ACC hyperexcitation thus led to the pain-related behaviours

What factors promote the ACC hyperexcitation following peripheral nerve injury? Lack of connections between excitatory and inhibitory neurons in ACC layer V associated with peripheral nerve damage (Blom et al., 2014) suggests that cortical disinhibition might result in potentiation of the intrinsic excitability of pyramidal neurons.

In this study, we provide the first evidence that unilateral SNI surgery induced TNF-α upregulation in contralateral ACC neurons (Fig. 3A and B), which distributed from layer IIupreg homogeneously (Fig. 7B, D) and co-localized with c-Fos positive cells (Fig. 4B). The induction of post-LTP in ACC is NMDA receptor-dependent (Zhuo, 2016), and this form of LTP is characterized by postsynaptic AMPA receptor modification or trafficking/insertion (Chen et al., 2014b; Toyoda et al., 2009). In ACC, nerve injury results in upregulation of NMDA receptor subunit NR2B, to a greater extent in the contralateral compared to the ipsilateral side; inhibiting contralateral NR2B by miRNA treatment can attenuate neuropathic pain (Ding et al., 2017). TNF-α is able to upregulate AMPA and NMDA receptors in some brain regions (Beattie et al., 2002; Stellwagen et al., 2005; Wei et al., 2008), and induce spinal or hippocampal LTP production in rats with nerve injury, leading to neuropathic pain (Liu et al., 2007) or pain-related memory deficits (Ren et al., 2011), respectively. Therefore, ACC TNF-α may be an upstream regulator promoting ACC hyperexcitability by increasing NMDA receptor activity. In our work, we found that TNF-α upregulation in the ACC contralateral side from PO 5d to 14d (Fig. 3C) was delayed relative to ipsilateral mechanical allodynia (PO 1d to 14d, Fig. 3D), and preceded late phase c-Fos upregulation after SNI (PO 7d and 10d, Fig. 1C and Fig. 4B, C). More importantly, neutralizing endogenous TNF-α in the ACC by injecting TNF-α antibody (200 μg/ml, 10 μl) blocked c-Fos upregulation and inhibited the decrease of paw withdrawal threshold to mechanical stimuli in SNI rats (Fig. 5D, H), showing that ACC TNF-α was involved in supraspinal mechanisms underlying the maintenance of neuropathic pain.

Drugs or genetic manipulations that block postsynaptic activity (post-LTP) in the ACC are sufficient to reduce or abolish behavioral sensitization, but do not affect negative emotions (Gao et al., 2016; Wang et al., 2011). The pre-LTP is linked to pain-related anxiety (Kim et al., 2011; Koga et al., 2015). ACC TNF-α can enhance synaptic efficacy through the increased probability of neurotransmitter release after peripheral inflammation (Jia et al., 2007), similar to the induction of pre-LTP. Here, TNF-α antibodies in two different doses were delivered into the ACC, and both doses were able to eliminate the pain aversion induced by CPA following SNI surgery (Fig. 5E, G), indicating the pivotal role of ACC TNF-α in pain aversive information processing. However, as shown in Fig. 3 and Supplementary Fig. 2, SNI-induced TNF-α expression was increased in other cortical areas including M2/M1 and administration of anti-TNF-α (200 μg/ml, 10 μl) antibody into M2/M1 inhibited the induction of mechanical allodynia and pain aversion by SNI. To test whether DREADD and/or drug injections might have leaked into these areas, we injected pontamine sky blue (2 μl) into the ACC (Supplementary Fig. 3). We found that this dye substantially remained in the ACC area with very little leakage. A small dose of injection could not completely exclude the possibility of drug leakage to other regions. However, given the viral transfection efficiency and/or the concentration at which the drugs acted, we believe that the drugs used in this work were primarily acting on the ACC to modulate pain behaviours. It has been reported that motor cortex is involved in the regulation of neuropathic pain (Kim et al., 2016; Kisler et al., 2017). The role of TNF-α in neuropathic pain in the motor cortex will be discussed and explored in our future work.

TNF-α may also mediate activities of voltage-gated sodium channels (Chen et al., 2011; He et al., 2010; Masocha, 2016) and dopamine (Wu et al., 2014) that may also be involved in the modulation of ACC excitability. The expression of dopaminergic receptors is altered in the ACC following sciatic denervation (Ortega-Legaspi et al., 2011). ACC dopamine can inhibit the glutamate mediated excitatory post-synaptic currents (EPSCs) in pyramidal neurons of layer II/III (Darvish-Ghane et al., 2016) and delivering dopamine into the ACC diminishes nociceptive behavior in a neuropathic pain model (Lopez-Avila et al., 2004). SNI-induced TNF-α in the nucleus accumbens reduces dopamine by increasing levels of dopamine transporter (Wu et al., 2014), another potential mechanism by which ACC TNF-α may contribute to descending facilitation through interacting with the dopaminergic system.

4.3. Effect of ACC neuronal activities on TNF-α expression

By recording calcium activities of ACC pyramidal neurons in awake mice, the hyperactivities of bilateral ACC are confirmed to be responsible for the development of neuropathic pain (Zhao et al., 2018). In our study, we also found that stimulating one side of ACC pyramidal neurons by DREADD-Gq without any nerve injury increased c-Fos and TNF-α protein levels on both sides of ACC (Fig. 6), which occurred in parallel to the bilateral mechanical allodynia observed in Fig. 2C. On the other hand, inhibiting the activity of ACC by DREADD-Gi significantly decreased c-Fos and TNF-α upregulation induced by SNI (Fig. 6), indicating that activation of ACC pyramidal neurons induced pain sensitization through promoting ACC TNF-α expression. However, as shown in Fig. 1 and Fig. 3, c-Fos expression level was first increased at PO 1 h and 1d while TNF-α was increased at PO 5d after SNI. No immediate change of TNF-α was found. Peripheral nerve injury-induced early self-protective mechanisms such as upregulation of anti-inflammatory cytokines (Shen et al., 2013; Yang et al., 2018) may play a role in such cascade. Cytokines involved in pain regulation can be broadly classified as proinflammatory cytokines IL-1β, TNF-α and anti-inflammatory cytokines IL-4, IL-10. Downregulation of anti-inflammatory cytokines and up-regulation of pro-inflammatory cytokines have been demonstrated in patients with chronic neuropathic pain conditions, such as complex regional pain syndrome etc. (Uceyler et al., 2007; Uceyler et al., 2006). The activation of glial cells in dorsal root ganglia and spinal cord results in the release of both pro- and anti-inflammatory cytokines, the balance between which determines whether pain chronicity is established after nerve injury (Austin et al., 2010). For example, IL-10, an anti-inflammatory cytokine, can down-regulate proinflammatory cytokines and inhibit the ectopic spontaneous discharges of injured DRG induced by paclitaxel (Ledeboer et al., 2007; Krukowski et al., 2016). In this study, the self-protective

mechanisms underlying early development of neuropathic pain might explain why transient abnormality of c-Fos in the ACC early following SNI did not induce significant upregulation of TNF-α.

A positive interaction between negative emotions and pain in disease conditions has been reported (Wiech and Tracey, 2009; Yoshino et al., 2010) and interventions that reduce anxiety are beneficial for reducing pain in chronic pain patients (Wiech and Tracey, 2009). The induction of pain-related aversion by inflammatory nociceptive stimuli can trigger astrocytic reactions and TNF-α expression in the ACC (Lu et al., 2011). In our study, however, decreased paw withdrawal threshold induced by SNI was not affected by CPA (a method to induce pain aversion) (Fig. 7G). The absence of CPA effects on SNI-induced mechanical allodynia might be due to peripheral nerve injury that has induced a maximal upregulation of TNF–er, decreased paw withdrawal threshold pain aversion by CPA following SNI enhanced expression of c-Fos but not TNF-α in ACC deep layers V/VI, as compared to SNI treatment alone.

In behavioral tests, CPA-induced pain aversion after SNI was not observed until PO 10d (Fig. 5A, B), mirroring late phase increased c-Fos levels (Fig. 1C). Repeated and prolonged activation of ACC is required for the acquisition of stable aversive memory (Johansen and Fields, 2004). Persistent peripheral nociceptive inputs trigger synaptic plasticity in the ACC to regulate sensory and aversive components of chronic pain (Li et al., 2010). Our observations indicate that abnormal upregulation of TNF-α in ACC following peripheral nerve injury may mediate these processes.

Supplementary data to this article can be found online at https://doi.org/10.1016/j.nbd.2019.04.012.

Conflict of interest

The authors declare that they have no conflict of interests.

Acknowledgements

This work was supported by the National Natural Science Foundation of China (Grant No. 81870873 and 81371228), the Fundamental Research Funds for the Central Universities of China (Grant No. 16ykjc02) and the Scientific Research Foundation of Guangdong Province of China (Grant No. 2017A020215039).

References

Al-Amin, H., et al., 2011. Chronic dizocilpine or apomorphine and development of neuropathy in two animal models II: effects on brain cytokines and neurotrophins. Exp. Neurol. 228, 30–40.
Austin, P.J., et al., 2010. The neuro-immune balance in neuropathic pain: involvement of inflammatory immune cells, immune-like glial cells and cytokines. J. Neuroimmunol. 229, 26–50.
Beattie, E.C., et al., 2002. Control of synaptic strength by glial TNFalpha. Science 295, 2282–2285.
Blom, S.M., et al., 2014. Nerve injury-induced neuropathic pain causes disinhibition of the anterior cingulate cortex. J. Neurosci. 34, 5754–5764.
Cao, X.Y., et al., 2009. Characterization of intrinsic properties of cingulate pyramidal neurons in adult mice after nerve injury. Mol. Pain 5, 73.
Chaplan, S.R., et al., 1994. Quantitative assessment of tactile allodynia in the rat paw. J. Neurosci. Methods 53, 55–63.
Chen, X., et al., 2011. TNF-alpha enhances the currents of voltage gated sodium channels in uninjured dorsal root ganglion neurons following motor nerve injury. Exp. Neurol. 227, 279–286.
Chen, T., et al., 2014a. Postsynaptic potentiation of corticospinal projecting neurons in the anterior cingulate cortex after nerve injury. Mol. Pain 10, 33.
Chen, T., et al., 2014b. Postsynaptic insertion of AMPA receptor onto cortical pyramidal neurons in the anterior cingulate cortex after peripheral nerve injury. Mol Brain 7, 76.
Chen, S.X., et al., 2018a. Calpain-2 regulates TNF-alpha expression associated with neuropathic pain following motor nerve injury. Neuroscience 376, 142–151.
Chen, S.X., et al., 2018b. Early CALP2 expression and microglial activation are potential inducers of spinal IL-6 up-regulation and bilateral pain following motor nerve injury. J. Neurochem. 145, 154–169.
Chen, T., et al., 2018c. Top-down descending facilitation of spinal sensory excitatory transmission from the anterior cingulate cortex. Nat. Commun. 9, 1886.
Darvish-Ghane, S., et al., 2016. Dopaminergic modulation of excitatory transmission in the anterior cingulate cortex of adult mice. Mol. Pain 12.
del Rey, A., et al., 2011. Chronic neuropathic pain-like behavior correlates with IL-1beta expression and disrupts cytokine interactions in the hippocampus. Pain 152, 2827–2835.
Detloff, M.R., et al., 2008. Remote activation of microglia and pro-inflammatory cytokines predict the onset and severity of below-level neuropathic pain after spinal cord injury in rats. Exp. Neurol. 212, 337–347.
Ding, M., et al., 2017. The role of miR-539 in the anterior cingulate cortex in chronic neuropathic pain. Pain Med. 18, 2433–2442.
Gao, S.H., et al., 2016. Activation of mGluR1 contributes to neuronal hyperexcitability in the rat anterior cingulate cortex via inhibition of HCN channels. Neuropharmacology 105, 361–377.
He, X.H., et al., 2010. TNF-alpha contributes to up-regulation of Nav1.3 and Nav1.8 in DRG neurons following motor fiber injury. Pain 151, 266–279.
Heinricher, M.M., et al., 2009. Descending control of nociception: specificity, recruitment and plasticity. Brain Res. Rev. 60, 214–225.
Ikeda, H., et al., 2013. Astrocytes are involved in long-term facilitation of neuronal excitation in the anterior cingulate cortex of mice with inflammatory pain. Pain 154, 2836–2843.
Jia, D., et al., 2007. TNF-alpha involves in altered prefrontal synaptic transmission in mice with persistent inflammatory pain. Neurosci. Lett. 415, 1–5.
Johansen, J.P., Fields, H.L., 2004. Glutamatergic activation of anterior cingulate cortex produces an aversive teaching signal. Nat. Neurosci. 7, 398–403.
Johansen, J.P., et al., 2001. The affective component of pain in rodents: direct evidence for a contribution of the anterior cingulate cortex. Proc. Natl. Acad. Sci. U. S. A. 98, 8077–8082.
Kang, S.J., et al., 2017. Inhibition of anterior cingulate cortex excitatory neuronal activity induces conditioned place preference in a mouse model of chronic inflammatory pain. Korean J Physiol Pharmacol 21, 487–493.
Kim, S.S., et al., 2011. Neurabin in the anterior cingulate cortex regulates anxiety-like behavior in adult mice. Mol Brain 4, 6.
Kim, J., et al., 2016. Motor cortex stimulation and neuropathic pain: how does motor cortex stimulation affect pain-signaling pathways? J. Neurosurg. 124, 866–876.
Kisler, L.B., et al., 2017. Bi-phasic activation of the primary motor cortex by pain and its relation to pain-evoked potentials - an exploratory study. Behav. Brain Res. 328, 209–217.
Koga, K., et al., 2015. Coexistence of two forms of LTP in ACC provides a synaptic mechanism for the interactions between anxiety and chronic pain. Neuron 85, 377–389.
Koyama, T., et al., 1998. Nociceptive neurons in the macaque anterior cingulate activate during anticipation of pain. Neuroreport 9, 2663–2667.
Krukowski, K., et al., 2016. CD8+ T cells and endogenous IL-10 are required for resolution of chemotherapy-induced neuropathic pain. J. Neurosci. 36, 11074–11083.
Kuo, C.C., Yen, C.T., 2005. Comparison of anterior cingulate and primary somatosensory neuronal responses to noxious laser-heat stimuli in conscious, behaving rats. J. Neurophysiol. 94, 1825–1836.
Kuzumaki, N., et al., 2007. Chronic pain-induced astrocyte activation in the cingulate cortex with no change in neural or glial differentiation from neural stem cells in mice. Neurosci. Lett. 415, 22–27.
Ledeboer, A., et al., 2007. Intrathecal interleukin-10 gene therapy attenuates paclitaxel-induced mechanical allodynia and proinflammatory cytokine expression in dorsal root ganglia in rats. Brain Behav. Immun. 21, 686–698.
Li, X.Y., et al., 2010. Alleviating neuropathic pain hypersensitivity by inhibiting PKMzeta in the anterior cingulate cortex. Science 330, 1400–1404.
Liu, Y.L., et al., 2007. Tumor necrosis factor-alpha induces long-term potentiation of C-fiber evoked field potentials in spinal dorsal horn in rats with nerve injury: the role of NF-kappa B, JNK and p38 MAPK. Neuropharmacology 52, 708–715.
Liu, Y., et al., 2017. TNF-alpha differentially regulates synaptic plasticity in the Hippocampus and spinal cord by microglia-dependent mechanisms after peripheral nerve injury. J. Neurosci. 37, 871–881.
Lopez-Avila, A., et al., 2004. Dopamine and NMDA systems modulate long-term nociception in the rat anterior cingulate cortex. Pain 111, 136–143.
Lu, Y., et al., 2011. Pain-related aversion induces astrocytic reaction and proinflammatory cytokine expression in the anterior cingulate cortex in rats. Brain Res. Bull. 84, 178–182.
Ma, L.Q., et al., 2016. Visual and noxious electrical stimulus-evoked membrane-potential responses in anterior cingulate cortical neurons. Mol Brain 9, 82.
Masocha, W., 2016. Gene expression profile of sodium channel subunits in the anterior cingulate cortex during experimental paclitaxel-induced neuropathic pain in mice. PeerJ 4, e2702.
Miyamoto, K., et al., 2017. Role of microglia in mechanical allodynia in the anterior cingulate cortex. J. Pharmacol. Sci. 134, 158–165.
Narita, M., et al., 2006. Chronic pain-induced emotional dysfunction is associated with astrogliosis due to cortical delta-opioid receptor dysfunction. J. Neurochem. 97, 1369–1378.
Ning, L., et al., 2013. Chronic constriction injury induced long-term changes in spontaneous membrane-potential oscillations in anterior cingulate cortical neurons in vivo. Pain Physician 16, E577–E589.
Ortega-Legaspi, J.M., et al., 2011. Expression of the dopaminergic D1 and D2 receptors in the anterior cingulate cortex in a model of neuropathic pain. Mol. Pain 7, 97.
Ren, W.J., et al., 2011. Peripheral nerve injury leads to working memory deficits and dysfunction of the hippocampus by upregulation of TNF-alpha in rodents. Neuropsychopharmacology 36, 979–992.
Shen, K.F., et al., 2013. Interleukin-10 down-regulates voltage gated sodium channels in rat dorsal root ganglion neurons. Exp. Neurol. 247, 466–475.
Song, Q., et al., 2015. Minocycline does not affect long-term potentiation in the anterior

cingulate cortex of normal adult mice. Mol. Pain 11, 25.
Stellwagen, D., et al., 2005. Differential regulation of AMPA receptor and GABA receptor trafficking by tumor necrosis factor-alpha. J. Neurosci. 25, 3219–3228.
Tan, W., et al., 2015. Alleviating neuropathic pain mechanical allodynia by increasing Cdh1 in the anterior cingulate cortex. Mol. Pain 11, 56.
Toyoda, H., et al., 2009. Roles of the AMPA receptor subunit GluA1 but not GluA2 in synaptic potentiation and activation of ERK in the anterior cingulate cortex. Mol. Pain 5, 46.
Tsuda, M., et al., 2017. Neuronal and microglial mechanisms for neuropathic pain in the spinal dorsal horn and anterior cingulate cortex. J. Neurochem. 141, 486–498.
Uceyler, N., et al., 2006. Reduced levels of antiinflammatory cytokines in patients with chronic widespread pain. Arthritis Rheum. 54, 2656–2664.
Uceyler, N., et al., 2007. Differential expression patterns of cytokines in complex regional pain syndrome. Pain 132, 195–205.
Urban, M.O., Gebhart, G.F., 1999. Supraspinal contributions to hyperalgesia. Proc. Natl. Acad. Sci. U. S. A. 96, 7687–7692.
Urban, M.O., et al., 1999. Descending facilitatory influences from the rostral medial medulla mediate secondary, but not primary hyperalgesia in the rat. Neuroscience 90, 349–352.
Viviani, B., et al., 2003. Interleukin-1beta enhances NMDA receptor-mediated intracellular calcium increase through activation of the Src family of kinases. J. Neurosci. 23, 8692–8700.
Wang, H., et al., 2011. Identification of an adenylyl cyclase inhibitor for treating neuropathic and inflammatory pain. Sci. Transl. Med. 3, 65ra3.
Wei, F., et al., 2002. Genetic elimination of behavioral sensitization in mice lacking calmodulin-stimulated adenylyl cyclases. Neuron 36, 713–726.
Wei, X.H., et al., 2007. Peri-sciatic administration of recombinant rat TNF-alpha induces mechanical allodynia via upregulation of TNF-alpha in dorsal root ganglia and in spinal dorsal horn: the role of NF-kappa B pathway. Exp. Neurol. 205, 471–484.
Wei, F., et al., 2008. Supraspinal glial-neuronal interactions contribute to descending pain facilitation. J. Neurosci. 28, 10482–10495.
Wei, X.H., et al., 2012. Peri-sciatic administration of recombinant rat IL-1beta induces mechanical allodynia by activation of src-family kinases in spinal microglia in rats. Exp. Neurol. 234, 389–397.
Wei, X.H., et al., 2013. The up-regulation of IL-6 in DRG and spinal dorsal horn contributes to neuropathic pain following L5 ventral root transection. Exp. Neurol. 241, 159–168.
Wiech, K., Tracey, I., 2009. The influence of negative emotions on pain: behavioral effects and neural mechanisms. Neuroimage 47, 987–994.
Wu, L.J., Zhuo, M., 2008. Resting microglial motility is independent of synaptic plasticity in mammalian brain. J. Neurophysiol. 99, 2026–2032.
Wu, Y., et al., 2014. Upregulation of tumor necrosis factor-alpha in nucleus accumbens attenuates morphine-induced rewarding in a neuropathic pain model. Biochem. Biophys. Res. Commun. 449, 502–507.
Xu, H., et al., 2008. Presynaptic and postsynaptic amplifications of neuropathic pain in the anterior cingulate cortex. J. Neurosci. 28, 7445–7453.
Yang, J., et al., 2018. Upregulation of N-type calcium channels in the soma of uninjured dorsal root ganglion neurons contributes to neuropathic pain by increasing neuronal excitability following peripheral nerve injury. Brain Behav. Immun. 71, 52–65.
Yoshino, A., et al., 2010. Sadness enhances the experience of pain via neural activation in the anterior cingulate cortex and amygdala: an fMRI study. Neuroimage 50, 1194–1201.
Zang, Y., et al., 2011. Upregulation of Nav1.3 channel induced by rrTNF in cultured adult rat DRG neurons via p38 MAPK and JNK pathways. Chin. J. Phys. 54, 241–246.
Zang, Y., et al., 2015. Calpain-2 contributes to neuropathic pain following motor nerve injury via up-regulating interleukin-6 in DRG neurons. Brain Behav. Immun. 44, 37–47.
Zhang, F., et al., 2008. Selective activation of microglia in spinal cord but not higher cortical regions following nerve injury in adult mouse. Mol. Pain 4, 15.
Zhang, Q., et al., 2017. Chronic pain induces generalized enhancement of aversion. Elife 6.
Zhang, X.L., et al., 2018. Palmitoylation of delta-catenin promotes kinesin-mediated membrane trafficking of Nav1.6 in sensory neurons to promote neuropathic pain. Sci. Signal. 11.
Zhao, M.G., et al., 2006. Enhanced presynaptic neurotransmitter release in the anterior cingulate cortex of mice with chronic pain. J. Neurosci. 26, 8923–8930.
Zhao, R., et al., 2018. Neuropathic pain causes pyramidal neuronal hyperactivity in the anterior cingulate cortex. Front. Cell. Neurosci. 12, 107.
Zhuo, M., 2016. Neural mechanisms underlying anxiety-chronic pain interactions. Trends Neurosci. 39, 136–145.